The inositol requiring Enzyme 1 (IRE1α) RNAse inhibitor, 4μ8C, is also a potent cellular antioxidant.

Stanley M.H. Chan[2], Mark P. Lowe[4], Ashton Bernard[2,3], Alyson A. Miller[2,3], and Terence P. Herbert[1,2*]

[1]School of Pharmacy, College of Science, University of Lincoln, Brayford Pool, Lincoln, Lincolnshire, LN6 7TS, UK; [2]School of Health and Biomedical Sciences, RMIT University, Bundoora, VIC 3083, Australia; [3]Institute of Cardiovascular & Medical Sciences, BHF Glasgow Cardiovascular Research Centre, University of Glasgow, Glasgow G12 8TA, UK; [4] Department of Chemistry (Chemical Biology Group), University of Leicester, Leicester, LE1 7RH, UK.

* Corresponding author

Professor Terence P. Herbert

School of Pharmacy,

College of Science,

University of Lincoln,

Brayford Pool, Lincoln,

Lincolnshire. LN6 7TS.

UK.

tel: +44 (0)1522 823337

Email: therbert@lincoln.ac.uk

Abstract

Inositol Requiring Enzyme 1 alpha (IRE1α) is an ER-transmembrane endonuclease that is activated in response to ER stress as part of the unfolded protein response (UPR). Chronic activation of the UPR has been implicated in the pathogenesis of many common disease including diabetes, cancer and neurological pathologies such as Huntington's and Alzheimer's disease.

7-hydroxy-4-methyl-2-oxo-2H-chromene-8-carbaldehyde (4μ8C) is widely used as a specific inhibitor of IRE1α ribonuclease activity in mechanistic studies (IC50 of 6.89 μM in cultured cells). However, in this paper we showed that 4μ8C acts as a potent reactive oxygen species (ROS) scavenger both in a cell free assay and in cultured cells at concentrations lower than that widely used to inhibit IRE1α activity. We demonstrate that i*n vitro,* 4μ8C effectively decreases xanthine/xanthine oxidase catalysed superoxide production with an IC50 of 0.2 μM. In cultured endothelial and clonal pancreatic beta-cells, 4μ8C inhibits angiotensin II-induced ROS production with IC50s of 1.92 and 0.29 μM respectively. In light of this discovery, conclusions reached using 4μ8C as an inhibitor of IRE1α should be carefully evaluated. However, this unexpected off-target effect of 4μ8C may prove therapeutically advantageous for the treatment of pathologies that are thought to be caused by, or exacerbated by, both oxidative and ER stress such as endothelial dysfunction and/or diabetes.

Abbreviation list: 4μ8C (7-hydroxy-4-methyl-2-oxo-2H-chromene-8-carbaldehyde), ROS (reactive oxygen species), AngII (angiotensin II), ER (endoplasmic reticulum), IRE1 (inositol requiring enzyme 1), UPR (unfolded protein response), IC (Inhibitory concentration), MIN6 (Mouse insulinoma 6 cells), NOX (NADPH oxidases), AT1R (angiotensin type 1 receptor), XBP1 (X-box binding protein-1), PERK (PKR like ER Kinase), ATF6 (Activating

transcription factor 6), CM-H2DCFDA (5-(and-6)-chloromethyl-2′,7′-dichlorodihydrofluorescein diacetate), bEnd.3 (Mouse microvascular cerebral endothelial cells).

Introduction

The endoplasmic reticulum (ER) is the site for the synthesis and processing of secretory and membrane proteins. Perturbations in ER homeostasis that interfere with protein folding result in the activation of an adaptive response termed the Unfolded Protein Response (UPR) [1,2]. Chronic activation of the UPR has been implicated in many human pathologies including infectious, neurodegenerative, autoimmune, and metabolic conditions [3–5].

The UPR is classically mediated by three ER-transmembrane proteins: PKR-like ER kinase (PERK), activating transcription factor 6 (ATF6), and inositol requiring enzyme 1α (IRE1α). IRE1α senses perturbations in ER homeostasis via its luminal domain which results in a conformational change [6,7]. This in turn promotes oligomerisation and the activation of its cytoplasmic protein kinase and RNAse domain. Activation of IRE1α leads to the cleavage and subsequent ligation of the mRNA encoding the X-box transcription factor-1 (XBP1) resulting in a frame shift and the synthesis of a truncated and transcriptionally active spliced form of XBP1 (XBP1s) [8]. In an attempt to relieve ER stress, XBP1s enhances the transcription of genes important in facilitating protein folding including the ER chaperone glucose regulated protein 78 [6,9]. However, chronic IRE1α activation can lead to programmed cell death through the activation of multiple signalling pathways (e.g.[6,10–12]).

A number of small molecule inhibitors of IRE1α have been identified and characterised including 7-hydroxy-4-methyl-2-oxo-2H-chromene-8-carbaldehyde (4μ8C) [13]. 4μ8C is an aromatic aldehyde that binds to IRE1α's RNAse domain and inhibits its activity. This inhibitor has provided valuable insights into defining the mechanism of action of IRE1α in both cellular physiology and pathophysiology (e.g.[13–19]) . 4μ8C has also been used in animal studies [20] although its effectiveness *in vivo* is uncertain. A recent study investigating the effect of 4μ8C on insulin secretion has highlighted the potential of this inhibitor to have off-target effects [21].

Consistent with this, in this report we demonstrate that 4μ8C not only inhibits IRE1α but also acts as a potent scavenger of ROS both in cell free assays and in cultured cells. In the light of this discovery conclusions reached using 4μ8C as a specific IRE1α RNAse inhibitor should be carefully considered.

Experimental

Cell culture. Mouse Insulinoma 6 (MIN6) cells [22] were used between passages 25 and 35 at ~80% confluence and cultured as previously described [23]. Mouse microvascular cerebral endothelial cells, bEnd.3 [24] were used between passage 24-34 (ATCC CRL-2299) and cultured in Dulbecco's Modified Eagle Medium (Life Technology, Australia) supplemented with 10% fetal bovine serum (FBS; Bovogen Australia), at 37°C and 5% CO_2.

Quantification of superoxide in a cell-free enzyme system. The xanthine/xanthine oxidase cell-free assay coupled with 5 μmol/L lucigenin-enhanced chemiluminescence [25] was used to assess the superoxide scavenging properties of 4μ8C. Briefly, to initiate the reaction, xanthine oxidase (50mU/ml) was added to Krebs-Hepes solution (NaCl 99 mmol/L, KCl 4.7 mmol/L, KH2PO4 10 mmol/L, $MgSO_4$ 1.2 mmol/L, $NaHCO_3$ 25 mmol/L, glucose 11 mmol/L, $CaCl_2$ 2.5 mmol/L, and EDTA 0.026 mmol/L, pH 7.4) containing xanthine (100 μmol/L) and lucigenin (5μmol/L). Where indicated experiments were performed in the absence or presence of superoxide dismutase (SOD; 250U/ml), 4μ8C (3nM - 30μM), DMSO ((0.1%) vehicle for 4μ8C), or Tiron (0.3 – 3000μM). Superoxide counts were measured using a BMG Clariostar plate reader (BMG Labtech, Melbourne, Australia). Background counts were then subtracted, and the superoxide level was expressed as relative luminescence units (RLU).

Quantification of cellular superoxide levels. Superoxide levels were measured using L-012 (100 μmol/l) enhanced chemiluminescence as previously described [26]. Cells were plated on a 96-well Optiplate (PerkinElmer, Melbourne, Australia). Upon treatments, 20 μL of 1mol/l L-

012 (in Krebs-Hepes) was added per well in semi-darkness to give a final concentration of 100 µmol/l. After treatments superoxide counts were measured using a BMG Clariostar plate reader over 90 min (BMG Labtech, Melbourne, Australia; 45 cycles, 3 s per well). The accumulated luminescence counts obtained were subtracted from the corresponding vehicle control and expressed as RLU.

Measurement of intracellular ROS generation. Intracellular ROS generation was measured using the cell-permeable ROS detector 5-(and-6)-chloromethyl-2′,7′-dichlorodihydrofluorescein diacetate (CM-H2DCFDA) (Thermo Scientific Australia). Briefly, cells incubated in phenol-red free growth media were loaded with CM-H2DCFDA (10 µmol/L). The oxidation of CM-H2DCFDA was captured kinetically (Ex/Em: 485/528 nm) at 37°C for 90 min. ROS production is expressed as accumulated relative fluorescence units (RFU).

Statistical analysis Data are expressed as mean +/- SEM, unless otherwise stated. Data were analysed by one-way ANOVA followed by Tukey's post-hoc test for multiple comparison between means using Prism 6 (GraphPad Software, USA). Differences were considered statistically significant at $p < 0.05$.

Results

4µ8C is a potent superoxide scavenger in a cell free assay. While studying the role of angiotensin II (AngII), an inducer of ROS, in the development of beta cell dysfunction [26] we observed that the commonly used IRE1α inhibitor 7-hydroxy-4-methyl-2-oxo-2H-chromene-8-carbaldehyde (4µ8C) inhibited, not only the activation of IRE1α, but also PERK, indicating that 4µ8C may have off-target effects (unpublished observations). Many naturally occurring antioxidants are polyphenolic compounds that act as free radical scavengers [27]. As 4µ8C [13] (Figure 1a) is a polyphenolic compound it also has the potential to act as a free radical scavenger. To investigate this possibility, cell-free xanthine/xanthine oxidase assays were performed using the chemiluminescent probe lucigenin. As expected the addition of xanthine oxidase to a solution containing xanthine and lucigenin led to a rapid increase in superoxide levels (figure 1b), which was abolished in the presence of SOD. Thus confirming that the reaction between xanthine and xanthine oxidase generates superoxide [25]. Furthermore, the addition of 4µ8C alone (i.e. in the absence of xanthine oxidase) had no effect on relative luminescence (figure 1b). Next, we measured superoxide levels, in the presence or absence of either increasing concentrations of the IRE1α inhibitor 4µ8C or as a positive control, tiron, a classical ROS scavenger [28]. 4µ8C (3mM to 30µM) (Figure 1c) or tiron (0.3µM to 3mM) (Figure 1d) reduced superoxide levels generated by the xanthine/xanthine oxidase cell-free assay in a concentration-dependent manner. Tiron inhibited xanthine/xanthine oxidase superoxide production with an IC50 of $7.3x10^{-6}$M, whereas 4µ8C inhibited superoxide production with an IC50 of $2.0x10^{-7}$M (figure 1e). Therefore, 4µ8C is a more potent superoxide scavenger than tiron in this cell-free enzyme assay.

4µ8C inhibits angiotensin II-induced superoxide production in pancreatic beta-cells and brain endothelial cells. Angiotensin II (AngII) increases cellular superoxide production by activating the NADPH oxidases (NOX) via the angiotensin type 1 receptor (AT1R) [29]. Therefore, to determine whether 4µ8C also acts as an antioxidant in cells, the mouse pancreatic beta-cell line, MIN6, and the mouse cerebral endothelial cell line, bEnd3, were treated with AngII in the presence or absence of 4µ8C (30µM) or, as control, the AT1R antagonist irbesartan (IRB). Superoxide levels were then measured using the luminol-based chemiluminescent probe, L-012. As anticipated, AngII caused a significant increase in superoxide production in both MIN6 (Figure 2a) and bEnd3 cells (Figure 2b) relative to control and this was blocked by IRB (Figure 2a and b). Importantly, AngII-induced increase in superoxide, in both cell lines was effectively inhibited by 30µM 4µ8C (Figure 2a and b); a concentration that is commonly used to inhibit IRE1α's RNAse activity.

To formally demonstrate that AngII-generated superoxide production was through the activation of NOX rather than ER stress-induced IRE1α activation, MIN6 and bEnd.3 cells were treated with AngII in the presence or absence of two NOX inhibitors, diphenyleneiodonium (DPI) and apocynin [30](Figure 2c and d). AngII treatment caused an increase in superoxide production which was effectively inhibited by both of the NOX inhibitors. This provides evidence that AngII-induced superoxide was generated through the activation of NOX and not IRE1α activation.

4µ8C concentration-dependent inhibition of angiotensin II-induced superoxide production in MIN6 cells and bEnd.3 cells. To investigate the potency of 4µ8C at inhibiting AngII-induced ROS production in cells, MIN6 and bEnd.3 cells were treated with AngII in the presence of increasing concentrations of 4µ8C and superoxide production was measured using L-012 (Figure 3). The addition of 4µ8C led to the concentration-dependent inhibition of AngII-generated superoxide with an IC50 of approximately 1.92µM in MIN6 cells, (Figure 3a) and

0.293µM in bEnd.3 cells (Figure3b). As 4µ8C inhibits IRE1α in mammalian cultured cells with an IC50 of 6.89µM [13], 4µ8C antioxidant activity is more potent than it ability to inhibit IRE1α RNAse activity.

4µ8C inhibits AngII-induced ROS production in MIN6 and bEnd.3 cells. As further evidence that 4µ8C is an antioxidant in mammalian cells, MIN6 and bEnd.3 cells were treated with AngII in the presence and absence of 4µ8C and changes in intracellular ROS was detected using 2',7' –dichlorofluorescin diacetate (CM-H2DCFDA), a fluorogenic dye that reacts with hydroxyl, hydrogen peroxide, peroxynitrite, and to a lesser extent superoxide [31]. Because hydrogen peroxide is a downstream product of superoxide, CM-H2DCFDA fluorescence is often used to implicate superoxide production [31]. Using CM-H2DCFDA, we confirmed that AngII increases ROS production in both MIN6 cells (Figure 4a) and bEnd.3 cells (Figure 4b), and that this is inhibited by apocynin. Importantly, AngII stimulates ROS production was also inhibited by 4µ8C (30µM). Thus 4µ8C acts as a ROS scavenger in cultured mammalian cells.

Discussion

Cell-permeable low-molecular weight inhibitors are used extensively to understand the role of specific enzymes in cellular physiology. Unfortunately, these compounds often lack specificity and display multiple off target effects that can lead to the misinterpretation of data. Our data demonstrates that 4μ8C, at concentrations widely used to inhibit IRE1α activity, also acts as a potent ROS scavenger both in a cell free assay and in cultured cells. Importantly, no other studies have shown that 4μ8C acts as a ROS scavenger.

The IC50 values for scavenging ROS by 4u8C differed in the two cell types used in this study. Although this may reflect the relative ability of AngII to stimulate ROS in these cells, comparison of ROS production between different cell types is difficult due to differences in, for example, ROS detector probe loading into the cell. Regardless, the effectiveness of the IRE1α inhibitor as a ROS scavenger is likely to be dependent on the amount of ROS being generated. In cells, such as phagocytes, that generate high concentration of ROS, the IC50 of the inhibitor against IRE1α RNAse activity may be greater than its IC50 for scavenging ROS. Interestingly, 4u8C has been used in macrophages to provide evidence for the role of IRE1α in ROS-dependent killing of bacteria [32]. Whether some or all of the effects of 4u8C reported on ROS-dependent killing were mediated by the antioxidant properties of 4u8C, as demonstrated in the report, is unclear but again highlights the importance of this study. Recently, Sato *et al* examined the role of IRE1α on insulin secretion in pancreatic β-cells using 4u8C. They discovered that 4u8C inhibited insulin secretion even in cells lacking the IRE1α RNAse domain demonstrating that 4u8C is able to block insulin secretion independent of the IRE1α/XBP1 pathway [21]. Given the results presented in this report, it is possible that the inhibitory effects of 4u8C on insulin secretion are through the scavenging of ROS.

4μ8C ability to act as a potent ROS scavenger is likely due to its coumarin type conjugated structure (Figure 1a), which can enable stabilisation of the free radical either by donation of a hydrogen atom or an electron [33]. This stabilisation is a result of the numerous resonance forms that are possible once the 4μ8C radical is formed, i.e. the 4u8c radical is resonance delocalised.

This off-target effect is a particular problem for researchers interested in delineating the role of IRE1 in ER stress responses, as oxidative stress can induce ER stress and conversely ER stress can promote oxidative stress [1,34]. Despite the potential problems of interpreting data using 4μ8C, off-target effects of low molecular cell permeable inhibitors can be advantageous in a clinical setting. For example, Gleevec (Imatinib), initially developed as an inhibitor of BCR-Abl, was later found to also inhibits the c-kit and platelet-derived growth factor receptor-A. This off target effect proved advantageous in its use as a treatment of gastrointestinal stromal tumour (GIST) [35]. Given that we demonstrate that 4μ8C can also act as a potent antioxidant this may prove therapeutically advantageous for the treatment of pathologies that are thought to be caused by, or exacerbated by, both oxidative and ER stress e.g. endothelial dysfunction or diabetes [1,4,36–38]. Therefore it is possible that 4μ8C, or a more pharmokinetically favourable structural analogue, may prove to have therapeutic value against such diseases.

Acknowledgements.

Declarations of interest. The authors have nothing to declare.

Funding information. This work was supported by a RMIT University research development fund awarded to TPH.

Author contribution statement.

SMHC helped in study design, performed the experiments, analysed the data and contributed to the writing of the manuscript. AM and AB helped with the acquisition of data and provided scientific advice. MPL contributed to discussions and reviewed/edited the manuscript. TPH conceived and designed the experiments, contributed to the acquisition of data and data analysis, and wrote the manuscript.

Figure legends

Figure 1. The superoxide scavenging effects of 4µ8C. (a) The chemical structure of 4µ8C. (b) The effect of addition of xanthine oxidase (XO) to xanthine (XA) on superoxide levels in the presence and absence of superoxide dismutase (SOD; 250U) and the effect of 4µ8C (30µM) alone on luminescence. (c and d) Superoxide was generated from the xanthine/xanthine oxidase reaction in the presence or absence of (c) 4µ8C (3nM – 30µM) or Vehicle (DMSO), (d) Tiron (0.3µM – 3000µM) or vehicle (saline) (e) Concentration-inhibition curves for 4µ8C (solid circles) and Tiron (solid squares) respectively. In all cases, superoxide was detected using lucigenin-enhanced chemiluminescence. All results are expressed as the mean +/- S.E.M of at least five independent experiments.

Figure 2. Angiotensin II induced superoxide formation in cells is blocked by 4µ8C. (a) MIN6 cells or (b) bEnd.3 cells were treated with 100 nM AngII in the absence or presence of 30 µM 4u8C or IRB (100 nM). (c) MIN6 cells or (d) bEnd.3 cells were treated with 100 nM AngII in the absence or presence of diphenyleneiodonium (DPI; 10 µM) or apocynin (10 µM). In all cases the formation of superoxide was detected using L-012. The results are presented as the mean RLU + S.E.M of at least five independent experiments ** $p<0.01$ versus control, ††

p<0.01 for the compared groups.

Figure 3. Dose-dependent effects of 4µ8C on superoxide formation. (a) MIN6 and (b) bEnd.3 cells were stimulated with 100 nM AngII in the absence or presence of increasing concentration of 4u8C (3 nM-30 µM) and the results plotted as concentration-inhibition curves. The formation of superoxide was detected using L-O12 and the results presented as the mean +/- S.E.M of six independent experiments.

Figure 4. The intracellular free radicals scavenging effect of 4µ8C. (a) MIN6 and (b) bEnd.3 cells were stimulated with 100 nM AngII in the absence or presence of 30µM 4u8C or 10µM apocynin. The formation of intracellular free radicals was detected using CM-H2DCFDA. The results are presented as the mean + S.E.M of three independent experiments. ** p<0.01 vs control; †† p<0.01 for the compared groups.

References.

1 Herbert, T. P. T. P. and Laybutt, D. R. R. (2016) A Reevaluation of the Role of the Unfolded Protein Response in Islet Dysfunction: Maladaptation or a Failure to Adapt? Diabetes **65**.

2 Schroder, M. and Kaufman, R. J. (2005) The mammalian unfolded protein response. Annu Rev Biochem **74**, 739–789.

3 Zhao, L. and Ackerman, S. L. (2006) Endoplasmic reticulum stress in health and

disease. Curr Opin Cell Biol **18**, 444–452.

4 Schroder, M. and Kaufman, R. J. (2005) ER stress and the unfolded protein response. Mutat Res **569**, 29–63.

5 Hotamisligil, G. S. Endoplasmic reticulum stress and the inflammatory basis of metabolic disease. Cell **140**, 900–917.

6 Chen, Y. and Brandizzi, F. (2013) IRE1: ER stress sensor and cell fate executor. Trends Cell Biol. **23**, 547–55.

7 Credle, J. J., Finer-Moore, J. S., Papa, F. R., Stroud, R. M. and Walter, P. (2005) Inaugural Article: On the mechanism of sensing unfolded protein in the endoplasmic reticulum. Proc Natl Acad Sci U S A **102**, 18773–18784.

8 Yoshida, H., Matsui, T., Yamamoto, A., Okada, T. and Mori, K. (2001) XBP1 mRNA is induced by ATF6 and spliced by IRE1 in response to ER stress to produce a highly active transcription factor. Cell **107**, 881–91.

9 Lee, A.-H., Iwakoshi, N. N. and Glimcher, L. H. (2003) XBP-1 regulates a subset of endoplasmic reticulum resident chaperone genes in the unfolded protein response. Mol. Cell. Biol. **23**, 7448–59.

10 Oslowski, C. M., Hara, T., O'Sullivan-Murphy, B., Kanekura, K., Lu, S., Hara, M., Ishigaki, S., Zhu, L. J., Hayashi, E., Hui, S. T., et al. (2012) Thioredoxin-interacting protein mediates ER stress-induced β cell death through initiation of the inflammasome. Cell Metab. **16**, 265–73.

11 Maurel, M., Chevet, E., Tavernier, J. and Gerlo, S. (2014) Getting RIDD of RNA: IRE1 in cell fate regulation. Trends Biochem. Sci. **39**, 245–254.

12 Wu, J., He, G.-T., Zhang, W.-J., Xu, J. and Huang, Q.-B. (2016) IRE1α Signaling Pathways Involved in Mammalian Cell Fate Determination. Cell. Physiol. Biochem. **38**, 847–858.

13 Cross, B. C. S., Bond, P. J., Sadowski, P. G., Jha, B. K., Zak, J., Goodman, J. M., Silverman, R. H., Neubert, T. A., Baxendale, I. R., Ron, D., et al. (2012) The molecular basis for selective inhibition of unconventional mRNA splicing by an IRE1-binding small molecule. Proc. Natl. Acad. Sci. **109**, E869–E878.

14 Sato, H., Shiba, Y., Tsuchiya, Y., Saito, M. and Kohno, K. (2017) 4μ8C Inhibits Insulin Secretion Independent of IRE1α RNase Activity. Cell Struct. Funct. **42**, 61–70.

15 Nam, S. T., Park, Y. H., Kim, H. W., Kim, H. S., Lee, D., Lee, M. B., Kim, Y. M. and Choi, W. S. (2017) Suppression of IgE-mediated mast cell activation and mouse anaphylaxis via inhibition of Syk activation by 8-formyl-7-hydroxy-4-methylcoumarin, 4μ8C. Toxicol. Appl. Pharmacol. **332**, 25–31.

16 Storniolo, A., Raciti, M., Cucina, A., Bizzarri, M. and Di Renzo, L. (2015) Quercetin affects Hsp70/IRE1α mediated protection from death induced by endoplasmic reticulum stress. Oxid. Med. Cell. Longev. **2015**, 645157.

17 Cojocari, D., Vellanki, R. N., Sit, B., Uehling, D., Koritzinsky, M. and Wouters, B. G. (2013) New small molecule inhibitors of UPR activation demonstrate that PERK, but not IRE1α signaling is essential for promoting adaptation and survival to hypoxia. Radiother. Oncol. **108**, 541–7.

18 Ma, J. H., Wang, J. J., Li, J., Pfeffer, B. A., Zhong, Y. and Zhang, S. X. (2016) The Role of IRE-XBP1 Pathway in Regulation of Retinal Pigment Epithelium Tight Junctions. Invest. Ophthalmol. Vis. Sci. **57**, 5244–5252.

19 Takahashi, N., Kimura, A. P., Naito, S., Yoshida, M., Kumano, O., Suzuki, T., Itaya, S., Moriya, M., Tsuji, M. and Ieko, M. (2017) Sarcolipin expression is repressed by endoplasmic reticulum stress in C2C12 myotubes. J. Physiol. Biochem.

20 Qiu, H., Garcia-Barrio, M. T. and Hinnebusch, A. G. (1998) Dimerization by translation initiation factor 2 kinase GCN2 is mediated by interactions in the C-terminal ribosome-binding region and the protein kinase domain. Mol Cell Biol **18**, 2697–2711.

21 Sato, H., Shiba, Y., Tsuchiya, Y., Saito, M. and Kohno, K. (2017) 4μ8C Inhibits Insulin Secretion Independent of IRE1α RNase Activity. Cell Struct. Funct. **42**, 61–70.

22 Ishihara, H., Asano, T., Tsukuda, K., Katagiri, H., Inukai, K., Anai, M., Kikuchi, M., Yazaki, Y., Miyazaki, J. I. and Oka, Y. (1993) Pancreatic beta cell line MIN6 exhibits characteristics of glucose metabolism and glucose-stimulated insulin secretion similar to those of normal islets. Diabetologia **36**, 1139–45.

23 Moore, C. E., Omikorede, O., Gomez, E., Willars, G. B. and Herbert, T. P. (2011) PERK activation at low glucose concentration is mediated by SERCA pump inhibition and confers preemptive cytoprotection to pancreatic beta-cells. Mol Endocrinol **25**, 315–326.

24 Ku, J. M., Taher, M., Chin, K. Y., Barsby, T., Austin, V., Wong, C. H. Y., Andrews, Z. B., Spencer, S. J. and Miller, A. A. (2016) Protective actions of des-acylated ghrelin on brain injury and blood-brain barrier disruption after stroke in mice. Clin. Sci. (Lond). **130**, 1545–58.

25 Miller, A. A., Maxwell, K. F., Chrissobolis, S., Bullen, M. L., Ku, J. M., Michael De Silva, T., Selemidis, S., Hooker, E. U., Drummond, G. R., Sobey, C. G., et al. (2013)

Nitroxyl (HNO) suppresses vascular Nox2 oxidase activity. Free Radic. Biol. Med. **60**, 264–71.

26 Chan, S. M., Lau, Y.-S., Miller, A. A., Ku, J. M., Potocnik, S., Ye, J.-M., Woodman, O. L. and Herbert, T. P. (2017) Angiotensin II causes beta cell dysfunction through an ER stress induced pro-inflammatory response. Endocrinology.

27 Tsao, R. (2010) Chemistry and Biochemistry of Dietary Polyphenols. Nutrients **2**, 1231–1246.

28 Yamada, J., Yoshimura, S., Yamakawa, H., Sawada, M., Nakagawa, M., Hara, S., Kaku, Y., Iwama, T., Naganawa, T., Banno, Y., et al. (2003) Cell permeable ROS scavengers, Tiron and Tempol, rescue PC12 cell death caused by pyrogallol or hypoxia/reoxygenation. Neurosci. Res. **45**, 1–8.

29 Cheng, Q. and Leung, P. S. (2011) An update on the islet renin-angiotensin system. Peptides **32**, 1087–95.

30 Jaquet, V., Scapozza, L., Clark, R. A., Krause, K.-H. and Lambeth, J. D. (2009) Small-Molecule NOX Inhibitors: ROS-Generating NADPH Oxidases as Therapeutic Targets. Antioxid. Redox Signal. **11**, 2535–2552.

31 Dikalov, S., Griendling, K. K. and Harrison, D. G. (2007) Measurement of reactive oxygen species in cardiovascular studies. Hypertens. (Dallas, Tex. 1979) **49**, 717–27.

32 Abuaita, B. H., Burkholder, K. M., Boles, B. R. and O'Riordan, M. X. (2015) The Endoplasmic Reticulum Stress Sensor Inositol-Requiring Enzyme 1α Augments Bacterial Killing through Sustained Oxidant Production. MBio **6**, e00705.

33 Veselinović, J. B., Veselinović, A. M., Vitnik, Ž. J., Vitnik, V. D. and Nikolić, G. M.

(2014) Antioxidant properties of selected 4-phenyl hydroxycoumarins: Integrated in vitro and computational studies. Chem. Biol. Interact. **214**, 49–56.

34 Cao, S. S. and Kaufman, R. J. (2014) Endoplasmic Reticulum Stress and Oxidative Stress in Cell Fate Decision and Human Disease. Antioxid. Redox Signal. **21**, 396–413.

35 Radford, I. R. (2002) Imatinib. Novartis. Curr. Opin. Investig. Drugs **3**, 492–9.

36 Han, J., Song, B., Kim, J., Kodali, V. K., Pottekat, A., Wang, M., Hassler, J., Wang, S., Pennathur, S., Back, S. H., et al. (2015) Antioxidants Complement the Requirement for Protein Chaperone Function to Maintain β-Cell Function and Glucose Homeostasis. Diabetes **64**, 2892–904.

37 Kassan, M., Galan, M., Partyka, M., Saifudeen, Z., Henrion, D., Trebak, M. and Matrougui, K. (2012) Endoplasmic Reticulum Stress Is Involved in Cardiac Damage and Vascular Endothelial Dysfunction in Hypertensive Mice. Arterioscler. Thromb. Vasc. Biol. **32**, 1652–1661.

38 Leo, C.-H. and Woodman, O. L. (2015) Flavonols in the Prevention of Diabetes-induced Vascular Dysfunction. J. Cardiovasc. Pharmacol. **65**, 532–44.

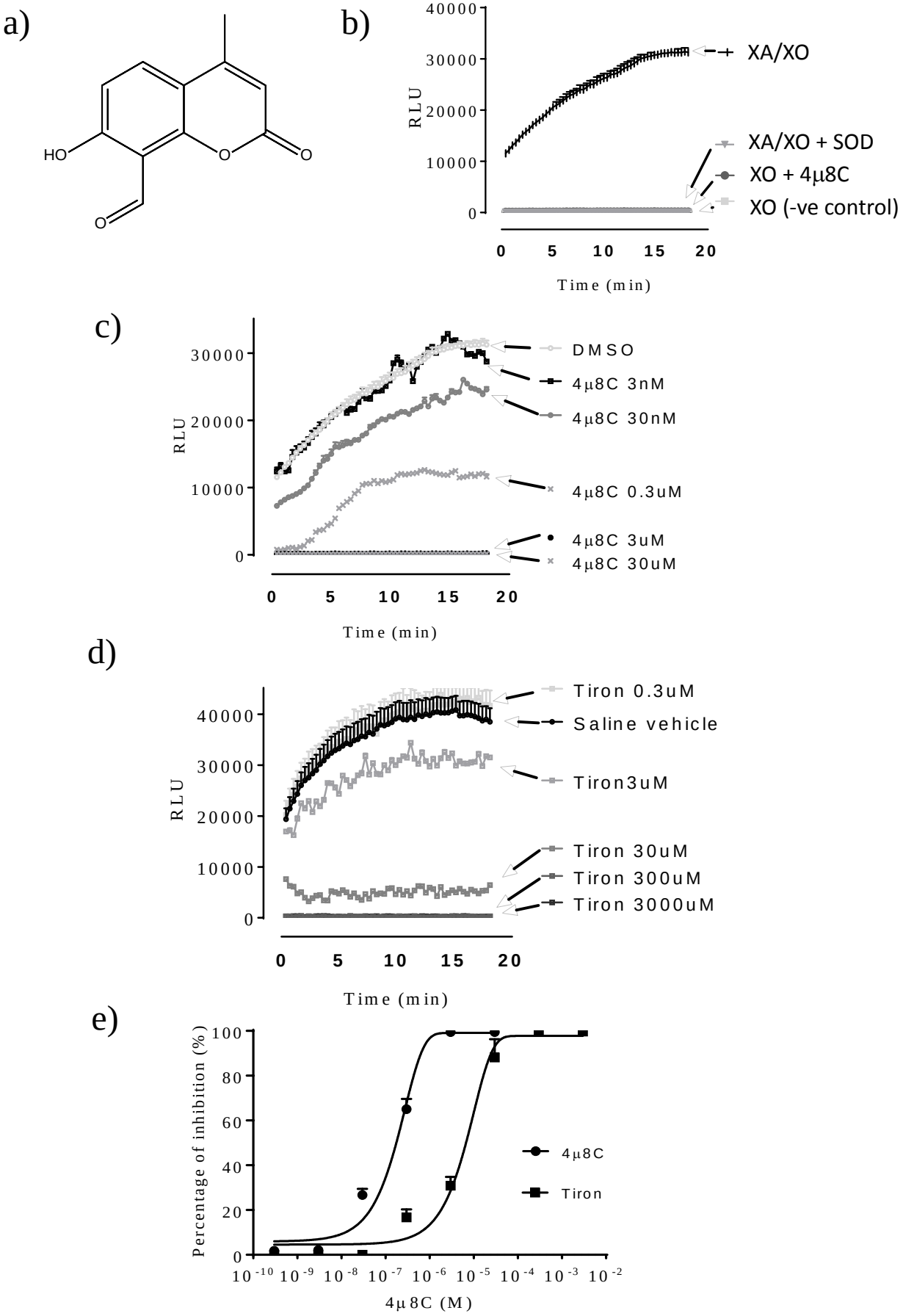
a)
HO
O
O
O
b)
RLU
40000
30000
20000
10000
0
0
5
10
15
20
Time (min)
XA/XO
XA/XO + SOD
XO + 4μ8C
XO (-ve control)
c)
RLU
30000
20000
10000
0
0
5
10
15
20
Time (min)
DMSO
4μ8C 3nM
4μ8C 30nM
4μ8C 0.3uM
4μ8C 3uM
4μ8C 30uM
d)
RLU
40000
30000
20000
10000
0
0
5
10
15
20
Time (min)
Tiron 0.3uM
Saline vehicle
Tiron3uM
Tiron 30uM
Tiron 300uM
Tiron 3000uM
e)
Percentage of inhibition (%)
100
80
60
40
20
0
10 -10 10 -9 10 -8 10 -7 10 -6 10 -5 10 -4 10 -3 10 -2
4μ8C (M)
4μ8C
Tiron

Figure 1

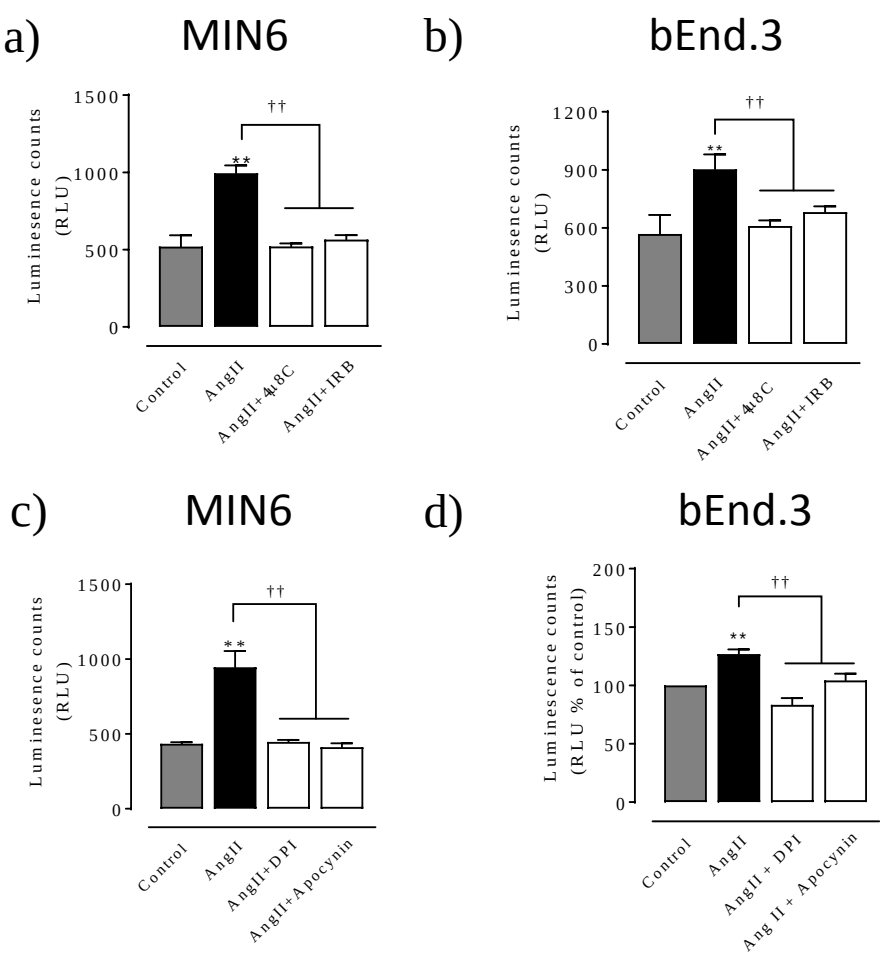
a)
MIN6
b)
bEnd.3
Luminescence counts (RLU)
1500
1000
500
0
1200
900
600
300
**
††
Control
AngII
AngII+4u8C
AngII+IRB
c)
MIN6
d)
bEnd.3
Luminescence counts (RLU)
Luminescence counts (RLU % of control)
200
150
100
50
AngII+DPI
AngII+Apocynin
AngII + DPI
Ang II + Apocynin

Figure 2

a) MIN6 b) bEnd.3

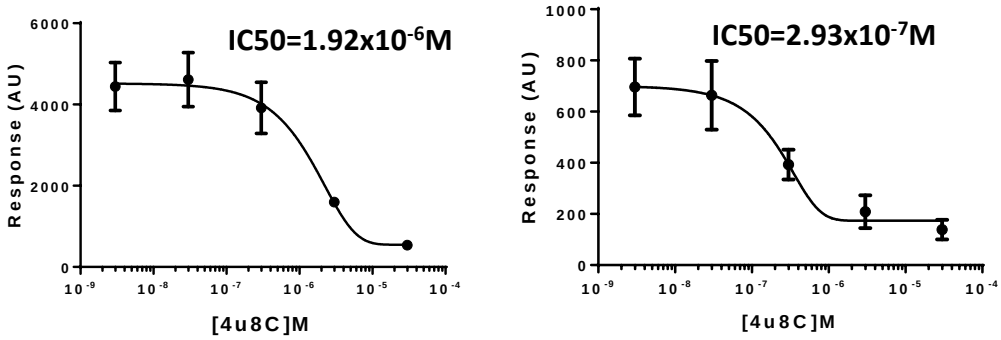

Figure 3

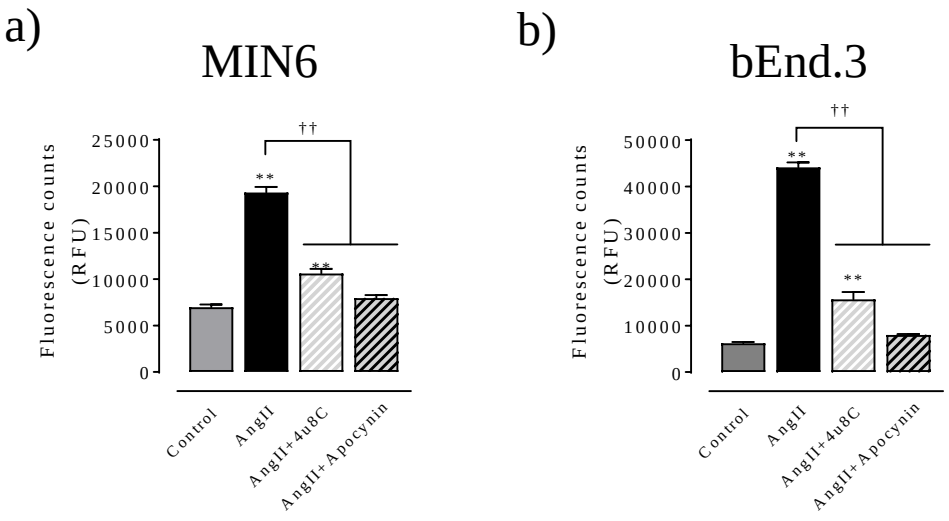
a)
MIN6
b)
bEnd.3
Fluorescence counts (RFU)
25000
20000
15000
10000
5000
0
50000
40000
30000
20000
10000
0
**
††
Control
AngII
AngII+4u8C
AngII+Apocynin

Figure 4